

First-principles study of the growth and diffusion of B and N atoms on the sapphire surface with h-BN as the buffer layer

Jianyun Zhao¹, Xu Li¹, Ting Liu¹, Yong Lu^{1,†}, and Jicai Zhang^{1,2,†}

¹College of Mathematics and Physics, Beijing University of Chemical Technology, Beijing 100029, China

²State Key Laboratory of Chemical Resource Engineering, Beijing University of Chemical Technology, Beijing 100029, China

Abstract: Currently, the preparation of large-size and high-quality hexagonal boron nitride is still an urgent problem. In this study, we investigated the growth and diffusion of boron and nitrogen atoms on the sapphire/h-BN buffer layer by first-principles calculations based on density functional theory. The surface of the single buffer layer provides several metastable adsorption sites for free B and N atoms due to exothermic reaction. The adsorption sites at the ideal growth point for B atoms have the lowest adsorption energy, but the N atoms are easily trapped by the N atoms on the surface to form N–N bonds. With the increasing buffer layers, the adsorption process of free atoms on the surface changes from exothermic to endothermic. The diffusion rate of B atoms is much higher than that of the N atoms thus the B atoms play a major role in the formation of B–N bonds. The introduction of buffer layers can effectively shield the negative effect of sapphire on the formation of B–N bonds. This makes the crystal growth on the buffer layer tends to two-dimensional growth, beneficial to the uniform distribution of B and N atoms. These findings provide an effective reference for the h-BN growth.

Key words: hexagonal boron nitride; buffer layer; first-principles calculations; molecular dynamics

Citation: J Y Zhao, X Li, T Liu, Y Lu, and J C Zhang, First-principles study of the growth and diffusion of B and N atoms on the sapphire surface with h-BN as the buffer layer[J]. *J. Semicond.*, 2021, 42(8), 082801. <http://doi.org/10.1088/1674-4926/42/8/082801>

1. Introduction

With the advancement of science and technology, the earlier materials can no longer meet the performance requirements of current devices very well. Since the Geim groups successfully separated graphene as a single atomic layer material in 2004^[1], a lot of graphene-like materials are drawing people's attention, which exhibit excellent physical and chemical performances. Hexagonal boron nitride (h-BN), as a wide bandgap semiconductor material sharing the similar crystal structure to graphite, is also destined to have great application potential and development prospects. The structure of h-BN is a six-membered cyclic honeycomb composed by B and N atoms alternately arranged, and its atomic layers overlap each other in a close-packed manner of AA'A... to form a crystal^[2]. The h-BN is called "white graphite" due to its white powder characteristics and the lattice difference between h-BN and graphite is only 1.7%^[3,4]. It has superior electrical insulation, thermal conductivity, corrosion resistance, good lubricity and chemical stability.

As a new type of wide-bandgap semiconductor material after gallium nitride (GaN) and aluminum nitride (AlN), h-BN shows excellent performance in many fields. Song *et al.* proved that the h-BN film exhibits significant deep ultraviolet absorption at a wavelength of 203 nm^[5], and Dahal *et al.* conducted electron beam excitation experiments on h-BN and found that the deep ultraviolet (DUV) region with 225

nm produced laser action^[6]. These phenomena prove the potential application of single crystal h-BN film in deep ultraviolet materials and as a deep ultraviolet chip-level semiconductor material. In the application of neutron detectors, Jiang *et al.* made metal–semiconductor–metal (MSM) neutrons detector by 0.3 μm thick h-BN. An obvious steady-state current response is produced after continuously irradiating the detector with the thermal neutron beam, which corresponds to the effective conversion efficiency of absorbed thermal neutrons close to 80%^[7,8]. All of this research has shown the great application potential of h-BN in the semiconductor field. However, it is still difficult to grow large-size single crystal h-BN thick films currently. Thus, in-depth research on the adsorption and diffusion of B and N atoms on the surface of the sapphire substrate can help people understand the micro growth mechanism of h-BN.

In this study, we use the *c*-plane sapphire (Al_2O_3) as the substrate, which is often used in the growth of h-BN by the chemical vapor deposition method. The h-BN buffer layer is introduced to improve the crystal growth. In this way, the growth of h-BN tends to be the two-dimensional growth, which can thus reduce the generation of the amorphous to improve the quality of h-BN. We systematically calculated and compared the adsorption energies of the free B and N atoms on the Al_2O_3 /h-BN-buffer-layer models. The diffusion behaviors of free B and N atoms on the buffer layer surface at different temperatures were also simulated to provide an effective guidance for h-BN growth in the experiment.

2. Calculation method

The first-principles calculations and molecular dynamics

Correspondence to: Y Lu, luy@mail.buct.edu.cn; J C Zhang, jczhang@mail.buct.edu.cn

Received 20 MARCH 2021; Revised 27 MARCH 2021.

©2021 Chinese Institute of Electronics

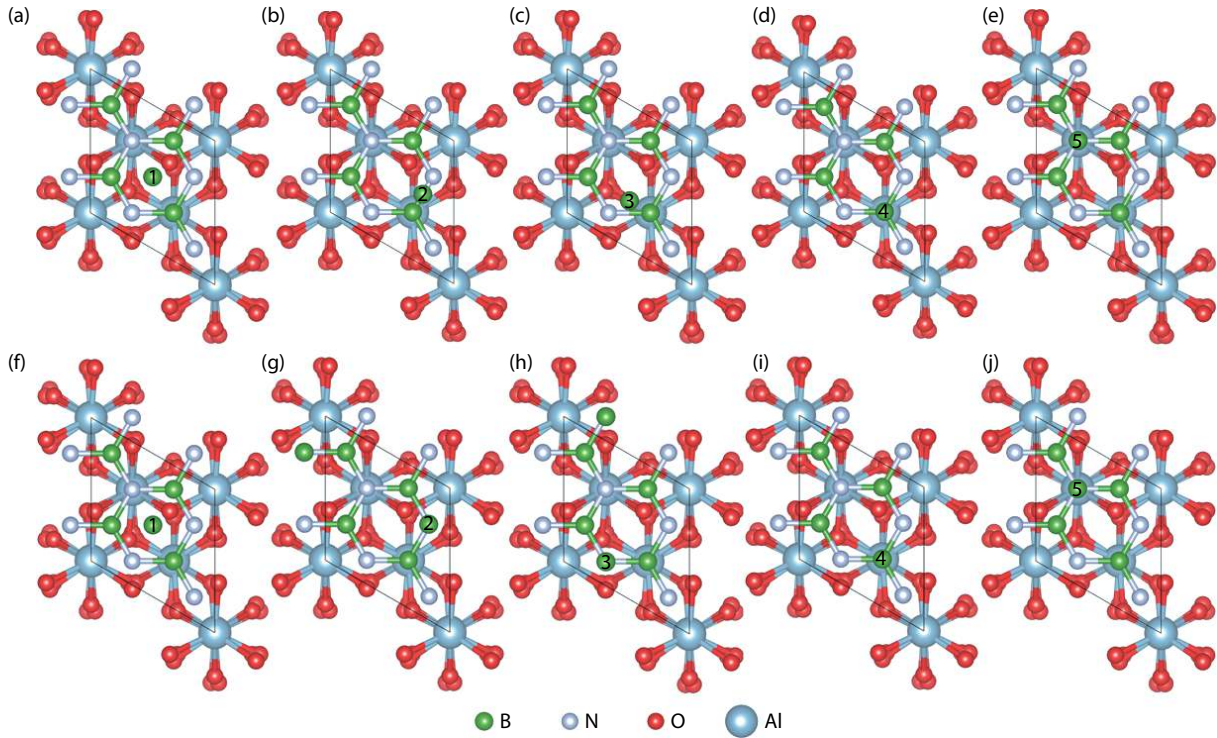


Fig. 1. (Color online) The top view of free B atoms at different adsorption sites with one h-BN buffer layer. (a–e) show the initial adsorption sites and (f–j) show the final configurations after optimization.

(MD) simulations of the growth and diffusion of B and N atoms on the surface of the $\text{Al}_2\text{O}_3/\text{h-BN}$ -buffer-layer were carried out based on the density functional theory (DFT) with the projection-enhanced wave (PAW) method as implemented in the VASP package^[9]. The electron exchange and correlation potential was described with the generalized gradient approximation with Perdew–Burke–Ernzerhof (PBE) form^[10]. The plane-wave cut-off energy was set to 400 eV. For the self-consistent formation energy calculations with the primitive cell, the $12 \times 12 \times 1$ k point mesh was used for the Brillouin zone integration^[11]. The convergence accuracies of the energy and force in the calculations are set to 1×10^{-5} eV and 0.02 eV/Å, respectively.

The lattice parameters are $a = 4.81$ Å and $c = 13.11$ Å for Al_2O_3 and $a = 2.51$ Å and $c = 7.19$ Å for h-BN, consisting well with the experimental results of $a = 4.76$ Å and $c = 12.99$ Å for Al_2O_3 and $a = 2.504$ Å and $c = 6.669$ Å for h-BN^[12, 13]. After optimizing the h-BN and Al_2O_3 primitive cells, we constructed (001) h-BN and (001) Al_2O_3 with different layers and combined them into a heterojunction structure, and h-BN was using the $2 \times 2 \times 1$ supercell. In order to prevent the influence on the surface and the bottom caused by the periodicity of the model, a vacuum layer of 15 and 10 Å was introduced on the surface and the bottom respectively. Since h-BN and graphite have a very similar hexagonal structure, we selected four adsorption sites based on the high symmetry point of graphite when selecting the adsorption sites of free B and N atoms, and we also selected the fifth adsorption site considering other adsorption possibilities^[14, 15]. The adsorption energy of the B and N atoms on the adsorption sites can be calculated by the following formula^[16–18]:

$$E_{\text{ads}} = E_{\text{all}} - E_{\text{part}} - E_{\text{atom}}, \quad (1)$$

where E_{ads} is the adsorption energy of atoms at the adsorp-

tion site, E_{all} and E_{part} are the total energy of the overall model and the total energy of the model without free atoms. E_{atom} is the single-atom energy of free B and N atoms, and the smaller the E_{ads} value, the easier to adsorb at this site. In the simulation process, we used different adsorption sites and different numbers of buffer layer to calculate the formation energy. The atomic positions and cell volume of $\text{Al}_2\text{O}_3/\text{h-BN}$ -buffer-layer were fixed, and only the free B or N atoms on the surface were optimized.

For the first-principles molecular dynamics (MD) simulations of the adsorption and diffusion of B and N atoms on the surface, the simulated temperature were set to the room temperature (~ 300 K) and the high temperature of 1300 °C (1573 K), respectively. The canonical ensemble (NVT) was used for all the MD simulations and the temperature was controlled by Nosé thermostat^[19]. The simulation time is 10 ps with the time step of 1 fs. The process can be monitored by the atomic coordinates generated by the MD simulations. We can characterize the diffusion behavior of free B and N atoms by calculating the mean square displacement (MSD) and diffusion coefficient D ^[20, 21].

$$\text{MSD} = \overline{r^2(t)} = \frac{1}{N} \left\langle \sum_{i=1}^N |r_i(t) - r_i(0)|^2 \right\rangle, \quad (2)$$

where $r_i(t)$ is the displacement of the i -th ion at time t , N is the total number of atoms, and the bracket represents the average over t . The variation of MSD with time is used to characterize the diffusion behavior of free B and N atoms on the surface. The relationship between MSD and diffusion coefficient D is as follows^[22–24]:

$$D = \frac{1}{2Nd\Delta t} \sum_{i=1}^N \left\langle |r_i(t + \Delta t) - r_i(t)|^2 \right\rangle_t = \frac{\text{MSD}(\Delta t)}{2d\Delta t}, \quad (3)$$

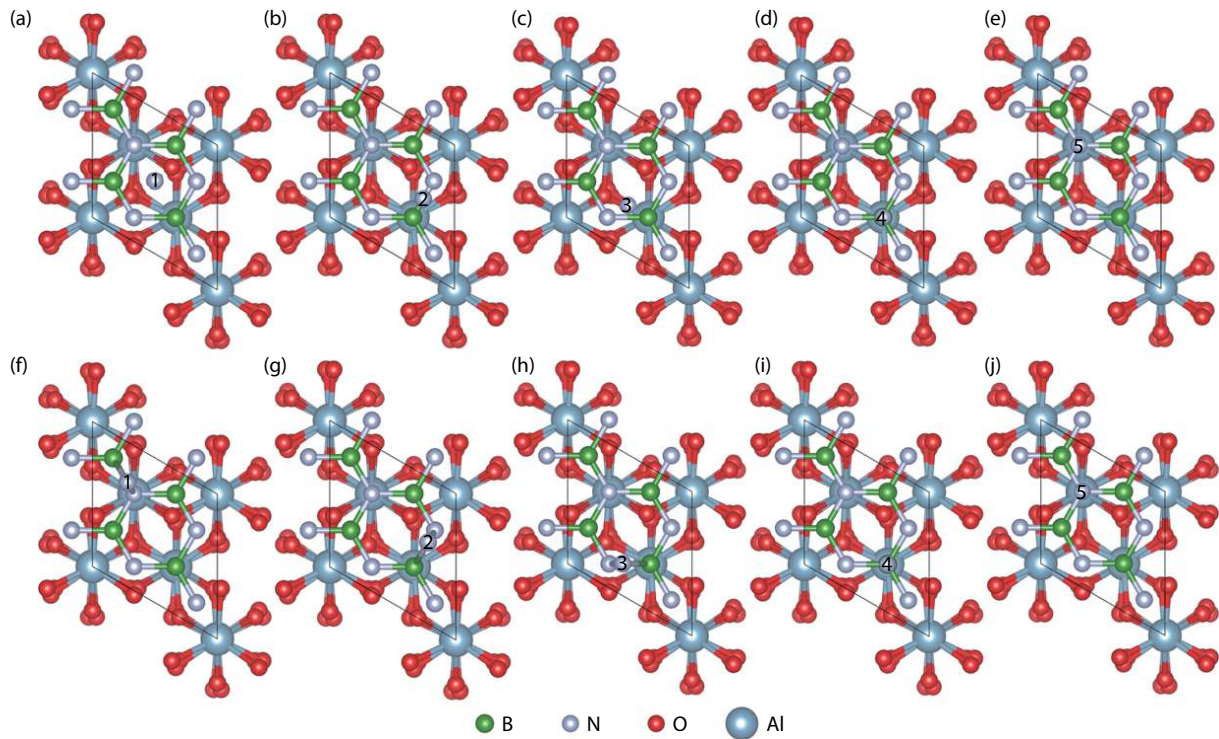


Fig. 2. (Color online) The top view of free N atoms at different adsorption sites with one h-BN buffer layer. (a–e) show the initial adsorption sites and (f–j) show the final configurations after optimization.

Table 1. The formation energies (eV) of free B or N atoms at the surface sites of the $\text{Al}_2\text{O}_3/\text{h-BN}$ -buffer-layer model.

Free atom	S1 (S_C)	S2	S3	S4 ($S_{B\text{-top}}$)	S5 ($S_{N\text{-top}}$)
B	-0.87	-1.11	-1.11	-0.76	-1.11
N	-2.05	-2.05	-2.05	-0.77	-2.02

where d is the dimensionality of the system (integer, $1 \leq d \leq 3$).

3. Results and discussions

The initial absorption models of the free state B and N atoms at different absorption sites and the structures after the relaxation optimization of the surface atomic positions are shown in Fig. 1 and Fig. 2, respectively, where the five potential adsorption sites, i.e., S1–S5, are marked with numbers. All models adopt the heterojunction composed of Al_2O_3 (0001) plane with the same thickness and the single layer h-BN along the normal direction. After optimizing the positions of the free B and N atoms on the surface, three final adsorption sites were obtained for both cases. As shown in Table 1, for the free B atoms, the top site of N ($S_{N\text{-top}}$) with the adsorption energy of -1.11 eV is the most stable adsorption site, which is the ideal growth site for the close packed structure of h-BN. The central site of the h-BN six-membered ring (S_C) and the top site of B ($S_{B\text{-top}}$) are two meta-stable sites with the adsorption energies of -0.87 and -0.76 eV, respectively. We note that the S_C corresponds to the growth site of rhombohedral structure boron nitride (r-BN)^[25]. The formation energies are all negative, indicating the exothermic process of the adsorption of B atoms on these sites. For the free N atoms, the most stable adsorption site is the top site of N with a small deviation towards to one of the neighbor B atom ($S_{N\text{-top}}$), as shown in Figs. 2(f)–2(h). The adsorption energy of $S_{N\text{-top}}$ is -2.05 eV, which is slightly lower than that of

-2.02 eV for the ideal top site of N ($S_{N\text{-top}}$). In the $S_{N\text{-top}}$ ' site, the free N atom bonds with the N atoms in the buffer layer to form N–N bond with a bond length of 1.502 Å, which restricts the diffusion of the surface N atom to other growth sites. The ideal growth site for h-BN is the top site of B ($S_{B\text{-top}}$), which is a meta-stable site with the adsorption energy of -0.77 eV. By comparing the formation energies of free B and N atoms on the surface, the N atoms are more easily to be adsorbed on the $S_{N\text{-top}}$ ' site, which plays a negative role in the growth of h-BN. In contrast, although the adsorption capacity of B atoms is weaker than that of N atoms, they tend to combine into h-BN structure.

After calculating the relationship between the adsorption sites and the formation energy, we investigated the influence of the number of h-BN buffer layer on the formation energy. The $\text{Al}_2\text{O}_3/\text{h-BN}$ -buffer-layer models with different numbers of buffer layer are shown in Fig. 3 for B and Fig. 4 for N atoms respectively. The S_C site is chosen as the initial absorption site for the free B and N atoms. By structural relaxation, the adsorption energies with different buffer layers were gathered in Table 2, and the final adsorption positions of B and N atoms on the surface were shown in Fig. 3 and Fig. 4, respectively. In general, the formation energy increases as the number of buffer layer increases. For B atom, the adsorption site after relaxation is not changed as the number of buffer layer increases from 1 to 3. But for the N atom, the final adsorption site for the N atom is changed to the $S_{N\text{-top}}$ ' site only with 1 buffer layer. As the buffer layer increases to 2 or 3, the initial S_C site for N atom is not changed. Both for the B and N atoms, the adsorption energy increases gradually as the number of buffer layer increases. When the number of h-BN buffer layer increases to 3, the adsorption process changes from an exothermic reaction to an endothermic reaction. As is known, during the growth process of h-BN, adjacent B and N

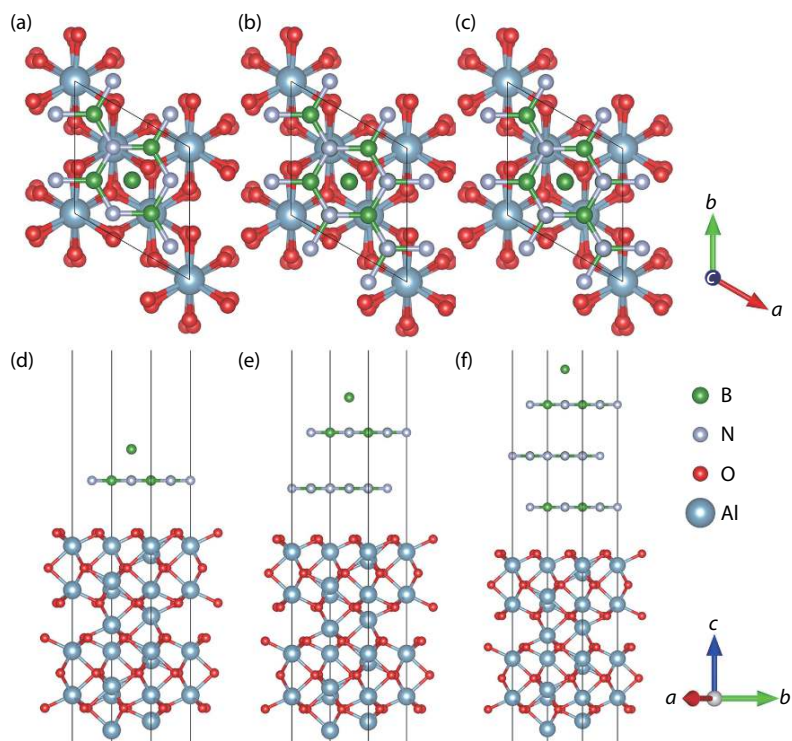


Fig. 3. (Color online) (a–c) The top view and (d–f) front view of the optimized adsorption positions for B atom on the surface with different buffer layers. The S_C site is chosen as the initial absorption site for the B atom.

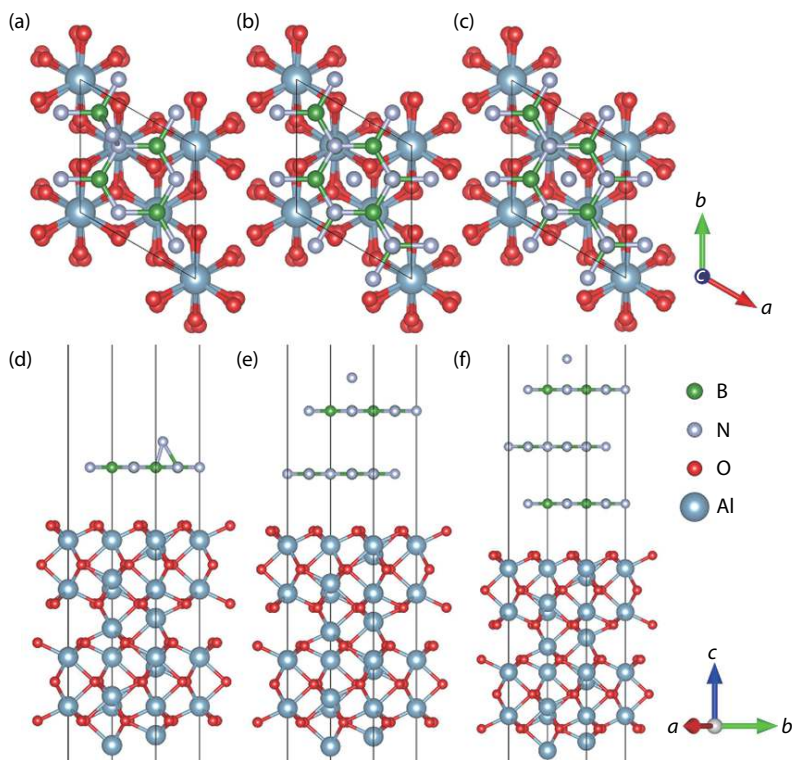


Fig. 4. (Color online) (a–c) The top view and (d–f) front view of the optimized adsorption positions for the N atom on the surface with different buffer layers. The S_C site is chosen as the initial absorption site for the B atom.

Table 2. The formation energies of free B and N atoms at the same position on the surface of the Al_2O_3/h -BN-buffer-layer model in a different number of buffer layers.

Parameter	1 buffer layer	2 buffer layers	3 buffer layers
B atom (eV)	-0.87	-0.14	0.01
N atom (eV)	-2.05	0.06	0.12

atoms in the same atomic layer are combined to form a B–N bond by sp^2 hybridization, and the inter layers are combined by van der Waals forces^[2]. According to the calculated results, it can be seen that the free B or N atom is affected by the coupling of Al_2O_3 and h-BN buffer layer. This coupling effect will be sharply weakened when the distance between ad-

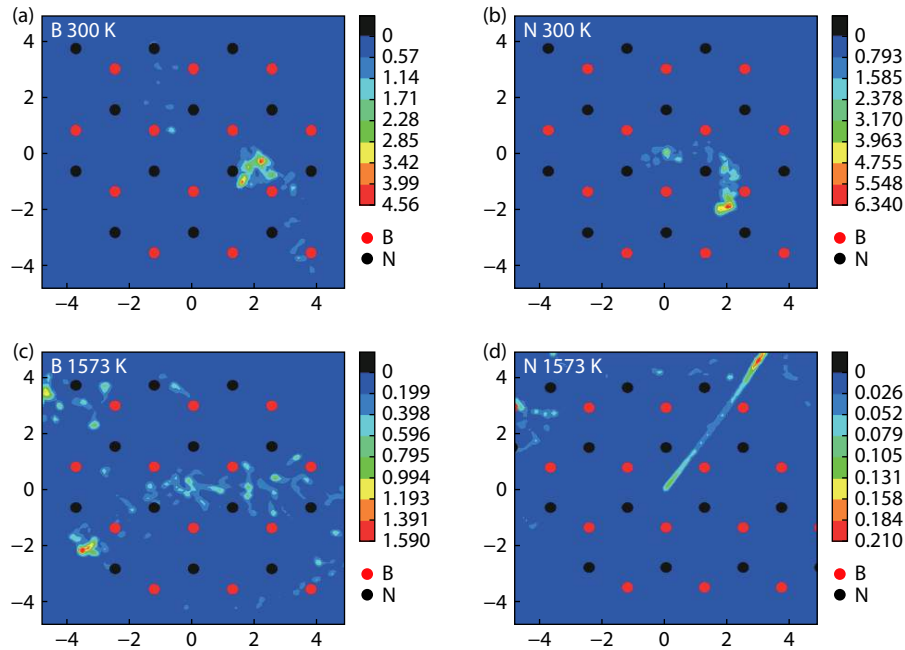


Fig. 5. (Color online) The probability distribution functions of atomic displacements projected onto the xy plane for (a) the B atom at 300 K, (b) the N atom at 300 K, (c) the B atom at 1573 K and (d) the N atom at 1573 K, respectively. The color scale indicates the distribution probability. The positions of B and N atoms of the buffer layer are marked.

sorption atom and the substrate increases. In previous experimental studies, it was found that N atoms can bond with Al and O atoms in the substrate when the nitriding process is applied to the surface of the sapphire substrate^[26, 27]. This indicates that Al_2O_3 has a strong adsorption effect on N atoms, which may cause the competition for forming an Al–N bond and B–N bond.

In addition to calculating the formation energy of one isolate B or N atom on the surface, we also set up a pair of free B and N atoms on the surface with one h-BN buffer layer. The calculated formation energy is -3.11 eV. Compared to the formation energies of isolate B and N atoms at their adsorption site, the formation energy of the coexisting B and N atoms are much lower, indicating that B and N atoms can interact with each other on the surface to form B–N bond. Namely, the free B and N atoms firstly bond with each other and then combine with the adsorption sites of the h-BN buffer layer.

The diffusion of free B and N atoms on the buffer layer surface was simulated by the first-principles molecular dynamics. The probability distribution functions of atomic displacements projected onto the xy plane is shown in Fig. 5 to trace the diffusion of B and N atoms in the surface. At room temperature, the B and N atoms both show a relative localization distribution. In general, the B and N atoms tend to diffuse around the $S_{\text{N-top}}$ site and $S_{\text{B-top}}$ site respectively by overcoming the energy barrier between the adjacent adsorption sites. As shown in Figs. 5(a) and 5(b), the trajectory of the N atom is more localized than that of B atom, which is more likely to jump between two adjacent adsorption sites. This can be compared quantitatively by calculating the MSD and diffusion coefficient of B and N atoms according to Eqs. (2) and (3). According to Fig. 6 and Table 3, the B atom has a larger MSD with respect to the N atom. As a result, the diffusion coefficient of B atom is 1.07×10^{-9} m^2/s at 300 K, much higher than 0.35×10^{-9} m^2/s of N atom. As temperature increases to 1573 K, the

activity of B and N atom are both increased and the distribution range is obviously expanded, as shown in Figs. 5(c) and 5(d). The diffusion of B atom is delocalized, which can diffuse freely on the surface by overcoming the energy barrier between the most stable and meta-stable sites. Although the distribution of N atom also shows delocalization characteristics, the trajectory is limited between specific adsorption sites. The N atom tends to diffuse across the sites around the B–N bond, increasing the probability of N bonding with N and B atoms in the buffer layer. The MSD of B atom is still larger than that of the N atom. The diffusion coefficients of B and N atoms at 1573 K increase to 17.04×10^{-9} and 7.18×10^{-9} m^2/s , respectively. The diffusion rate of B atom is much higher than that of the N atom. It can thus be concluded that B atoms play a leading role in the growth process of h-BN. At high temperature, B atoms distribute uniformly at the growth sites by diffusion, then promoting N atoms to the break away from the localization to form B–N bonds.

4. Conclusion

In summary, we studied the growth and diffusion of B and N atoms on the surface of the $\text{Al}_2\text{O}_3/\text{h-BN}$ -buffer-layer through first-principles calculations based on the density functional theory. The results show that the surface of single-buffer-layer h-BN provides several metastable adsorption sites for free B and N atoms due to the exothermic reaction. The free B atoms have the lowest adsorption energy at the adsorption site of the ideal growth point for h-BN, but the free N atoms are most easily to be trapped by the N atoms on the h-BN buffer layer to form the N–N bonds. As the number of buffer layer increases, the binding capacity of the surface of the buffer layer with free B and N atoms decreases. When the number of the h-BN buffer layer increases to three, the adsorption of the free B and N atoms on the surface changes from an exothermic reaction to an endothermic reaction. The influ-

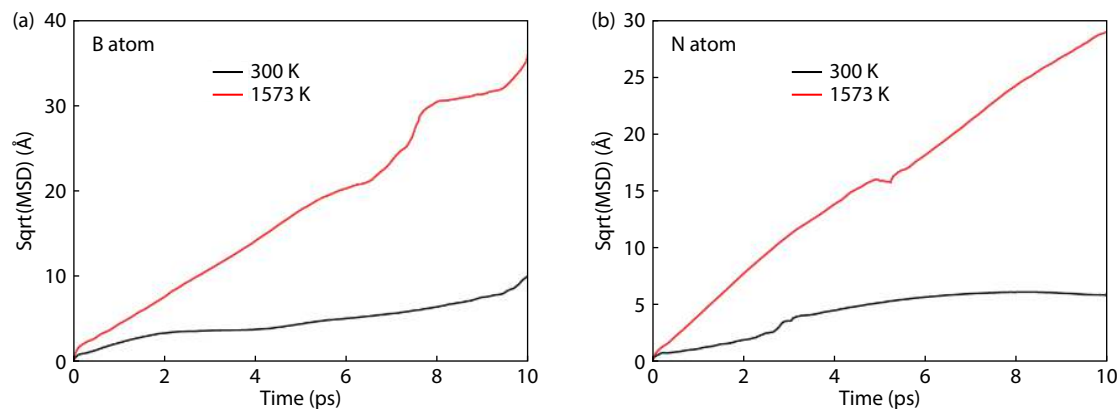


Fig. 6. The MSD curves of (a) B atoms and (b) N atoms on the buffer layer surface at different temperatures.

Table 3. Diffusion coefficients of free atoms on the surface of the model at different temperatures.

Free atom	T (K)	D (10^{-9} m ² /s)
B	300	1.07
	1573	17.04
N	300	0.35
	1573	7.18

ence of the Al_2O_3 substrate on the surface atoms is largely weakened. As temperature increases from 300 to 1573 K, the activity and diffusion range of B and N atoms increase significantly. The B atoms can diffuse freely on the buffer layer surface by overcoming the energy barrier between the adsorption sites. But the diffusion trajectory of N atoms is restricted in the specific adsorption sites around the B–N bonds of buffer layer. The B atoms play a major role in the formation of B–N bonds on the surface, the diffusion rate of which is much higher than that of the N atom. The introduction of buffer layers make the crystal growth have the characteristics of two-dimensional growth, which can effectively shield the negative effect of the substrate on the formation of B–N bonds. Also, they are conducive to the uniform diffusion surface B and N atoms, which can thus reduce the generation of the amorphous to improve the growth quality of h-BN.

Acknowledgements

This work was partly supported by the National Natural Science Foundation of China (61874007, 12074028), the Beijing Municipal Natural Science Foundation (4182046), Shandong Provincial Major Scientific and Technological Innovation Project (2019JZZY010209), Key-area research and the development program of Guangdong Province (2020B010172001), and the Fundamental Research Funds for the Central Universities (buctrc201802, buctrc201830, buctrc202127).

References

- Geim A K, Novoselov K S. The rise of graphene. *Nat Mater*, 2007, 6, 183
- Wang J G, Mu X J, Wang X X, et al. The thermal and thermoelectric properties of in-plane C-BN hybrid structures and graphene/h-BN van der Waals heterostructures. *Mater Today Phys*, 2018, 5, 29
- Tang Q, Zhou Z. Graphene-analogous low-dimensional materials. *Prog Mater Sci*, 2013, 58, 1244
- Wang J G, Ma F C, Sun M T. Graphene, hexagonal boron nitride, and their heterostructures: Properties and applications. *RSC Adv*, 2017, 7, 16801
- Song Y X, Zhang C R, Li B, et al. Triggering the atomic layers control of hexagonal boron nitride films. *Appl Surf Sci*, 2014, 313, 647
- Dahal R, Li J, Majety S, et al. Epitaxially grown semiconducting hexagonal boron nitride as a deep ultraviolet photonic material. *Appl Phys Lett*, 2011, 98, 211110
- Doan T C, Majety S, Grenadier S, et al. Fabrication and characterization of solid-state thermal neutron detectors based on hexagonal boron nitride epilayers. *Nucl Instrum Methods Phys Res Sect A*, 2014, 748, 84
- Jiang H X, Lin J Y. Hexagonal boron nitride for deep ultraviolet photonic devices. *Semicond Sci Technol*, 2014, 29, 084003
- Cai L C, Fan X H, Su H T, et al. First principles calculation of the lattice constants of hexagonal and cubic boron nitride to 3000 K and 30 GPa. *Ferroelectrics*, 2020, 566, 136
- Hafner J. Ab-initio simulations of materials using VASP: Density-functional theory and beyond. *J Comput Chem*, 2008, 29, 2044
- Chadi D J. Special points for Brillouin-zone integrations. *Phys Rev B*, 1977, 16, 1746
- Yang X, Nitta S, Nagamatsu K, et al. Growth of hexagonal boron nitride on sapphire substrate by pulsed-mode metalorganic vapor phase epitaxy. *J Cryst Growth*, 2018, 482, 1
- Chikh H, SI Ahmed F, Afir A, et al. *In-situ* X-ray diffraction study of alumina α - Al_2O_3 thermal behavior under dynamic vacuum and constant flow of nitrogen. *J Alloy Compd*, 2016, 654, 509
- Wu J H, Hagelberg F, Sattler K. First-principles calculations of small silicon clusters adsorbed on a graphite surface. *Phys Rev B*, 2005, 72, 085441
- Govind Rajan A, Strano M S, Blankschtein D. Ab initio molecular dynamics and lattice dynamics-based force field for modeling hexagonal boron nitride in mechanical and interfacial applications. *J Phys Chem Lett*, 2018, 9, 1584
- Zoroddu A, Bernardini F, Ruggerone P, et al. First-principles prediction of structure, energetics, formation enthalpy, elastic constants, polarization, and piezoelectric constants of AlN, GaN, and InN: Comparison of local and gradient-corrected density-functional theory. *Phys Rev B*, 2001, 64, 045208
- Shigemi A, Wada T. Enthalpy of formation of various phases and formation energy of point defects in perovskite-type NaNbO_3 by first-principles calculation. *Jpn J Appl Phys*, 2004, 43, 6793
- Petrushenko I K, Petrushenko K B. Stone-Wales defects in graphene-like boron nitride-carbon heterostructures: Formation energies, structural properties, and reactivity. *Comput Mater Sci*, 2017, 128, 243
- Nosé S. A unified formulation of the constant temperature molecular dynamics methods. *J Chem Phys*, 1984, 81, 511
- Wang V, Xu N, Liu J C, et al. VASPKit: A user-friendly interface facilit-

ating high-throughput computing and analysis using VASP code. arXiv: 1908.08269, 2019

- [21] Kowsari M H, Alavi S, Ashrafizaadeh M, et al. Molecular dynamics simulation of imidazolium-based ionic liquids. I. Dynamics and diffusion coefficient. *J Chem Phys*, 2008, 129, 224508
- [22] Sadki K, Zanane F Z, Ouahman M, et al. Molecular dynamics study of pristine and defective hexagonal BN, SiC and SiGe monolayers. *Mater Chem Phys*, 2020, 242, 122474
- [23] Nagai T, Tsurumaki S, Urano R, et al. Position-dependent diffusion constant of molecules in heterogeneous systems as evaluated by the local mean squared displacement. *J Chem Theory Comput*, 2020, 16, 7239
- [24] Manga V R, Poirier D R. Ab initio molecular dynamics simulation of self-diffusion in Al-Si binary melts. *Model Simul Mater Sci Eng*, 2018, 26, 065006
- [25] Chubarov M, Högberg H, Henry A, et al. Challenge in determining the crystal structure of epitaxial 0001 oriented sp²-BN films. *J Vac Sci Technol A*, 2018, 36, 030801
- [26] Skuridina D, Dinh D V, Pristovsek M, et al. Surface and crystal structure of nitridated sapphire substrates and their effect on polar InN layers. *Appl Surf Sci*, 2014, 307, 461
- [27] Dwikusuma F, Kuech T F. X-ray photoelectron spectroscopic study on sapphire nitridation for GaN growth by hydride vapor phase epitaxy: Nitridation mechanism. *J Appl Phys*, 2003, 94, 5656



Jianyun Zhao got his B.E. degree from Beijing University of Chemical Technology in 2018. Now he is a postgraduate student at Beijing University of Chemical Technology under the supervision of Prof. Jicai Zhang. He has been working in Wide Bandgap Semiconductor Materials and Devices Laboratory for Beijing University of Chemical Technology since 2018. His current research focuses on the growth and preparation of aluminum nitride and boron nitride.



Xu Li got his B.S. degree from Northeastern University in 2018. Now he is a postgraduate student at Beijing University of Chemical Technology under the supervision of Prof. Jicai Zhang. He has been working in Wide Bandgap Semiconductor Materials and Devices Laboratory for Beijing University of Chemical Technology since 2018. His current research focuses on the growth of aluminum nitride and boron nitride.



Ting Liu received her Ph.D. degree from University of Chinese Academy of Sciences in 2018. She was a postdoctor researcher in Nagoya University and National Institute for Materials Science in Japan from 2018 to 2020. In 2021, she joined the School of Mathematics and Physics in Beijing University of Chemical Technology as an Associate Professor. Her current research interests include Non-polar AlN, BN, AlGaIn-based deep ultraviolet LED and wearable technology research.



Yong Lu received the Ph.D. degree in Beijing Institute of Applied Physics and Computational Mathematics in 2014. He worked as a postdoctoral researcher in Beijing Computing Science Research Center from 2014 to 2016. He joined the college of mathematics and physics, Beijing University of Chemical Technology in 2016 and presently is the associate professor. His research interests mainly focus on the lattice dynamics, thermal transport properties, dynamic simulation of crystal growth, defects and doping in semiconductors.



Jicai Zhang received the B.S. degree in physics from Qufu Normal University in 1997, the M.S. degree in condensed matter physics from Peking University in 2001, and the Ph.D. degree in microelectronics and solid-state electronics from the Institute of Semiconductors, CAS, in 2005. From 2005 to 2017, he was with Technion-Israel Institute of Technology, Israel, Nagoya Institute of Technology and Mie University, Japan, Suzhou Institute of Nano-Tech and Nano-Bionics, CAS, China, respectively. Since 2017, he has been with Beijing University of Chemical Technology as a Professor. His current research focused on group-III nitrides and related devices.